THE NTH-ROOT STACK: A CHEAP AND EFFECTIVE PROCESSING TECHNIQUE

P. L. McFadden, B. J. Drummond and S. Kravis

Geophysical data are typically very noisy, so multichannel observations are usually made and these data stacked in order to extract the signal. Compared with subsequent processing of the data, there is rarely very much thought put into the stacking process, yet this is a crucial step. If the stacking process used is not optimum for the particular application of the data, information will have been lost or obscured and no amount of subsequent processing can recover it.

The most common stack is the simple linear stack, which is merely the arithmetic mean of the individual observations. If the noise is Gaussian, then the linear stack is statistically optimal: it is both linear and unbiased and it has the smallest variance of any linear, unbiased estimator. On this basis it is widely used as a standard stacking procedure.

Unfortunately, seismic data are often not well-behaved, and the noise distribution is frequently non-Gaussian. One of the major problems is the presence of noise spikes (i.e. one or more of the observations is substantially in error), and the simple linear stack is notorious for its poor behaviour in the presence of such spikes. In order to overcome this fundamental problem stacks such as the α-trimmed stack, the median stack, and the weighted stack are often used. Each of these stacks is relatively expensive in computing time (the observations have to be ordered for the α-trimmed and median stacks, and an iterative procedure is required to determine the best weights for the weighted stack) but there is an enormous gain in resistance to noise spikes.

Although these stacks overcome the problem of noise spikes, they do not in fact address the fundamental question of what is the best stacking process for the particular application. Although one might intuitively feel that it is desirable for a stack to be linear and unbiased, this is not necessarily the case. For example, in many seismic applications it is of crucial importance to be able to identify reliably those portions of a record where a genuine response exists, and if so, when it arrived. Under such circumstances linearity and lack of bias are unimportant. Consequently it is very important to decide a *priori* precisely what is required of the stack, and so determine whether linearity and lack of bias are appropriate. If they are not necessary, one should seriously consider nonlinear stacking techniques, since they provide much greater flexibility and often provide a better result.

The Nth-root stack is nonlinear and has some very interesting and powerful characteristics. If we have m observations t_i then the result R_N of an Nth-root stack of these observations is defined by

$$R_N = \left[\frac{1}{m} \sum_{i=1}^{m} \sqrt[N]{t_i} \right]^N$$

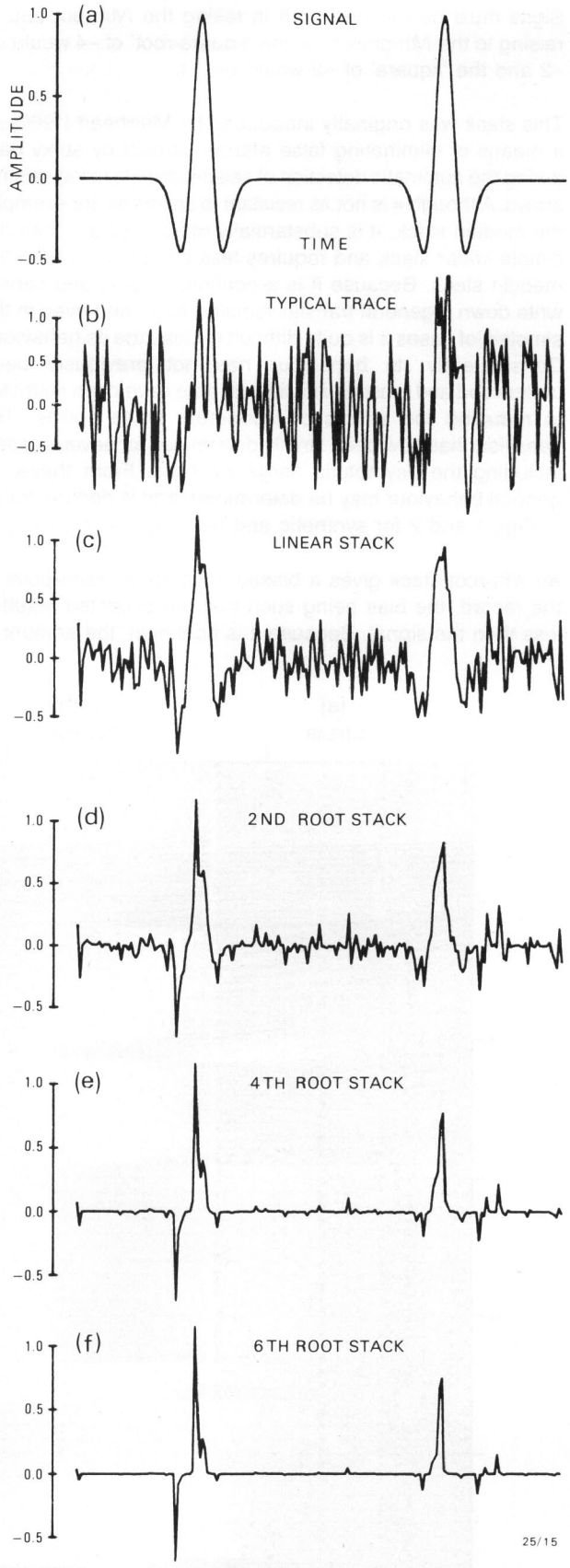

FIGURE 1

1a shows a trace in which the signal is represented by two identical wavelets. Twelve such traces were generated and random noise added to each; an example of a noisy trace is shown in 1b. The traces were then stacked using linear, 2nd-, 4th- and 6th-root stacks (1c, 1d, 1e and 1f resp.).

Signs must be retained both in taking the *N*th-root and in raising to the *N*th-power, i.e. the 'square-root' of −4 would be −2 and the 'square' of −2 would be −4.

This stack was originally introduced by Muirhead (1968) as a means of eliminating false alarms caused by spiky data during the automatic detection of seismic events using seismic arrays. Although it is not as resistant to spikes as, for example, the median stack, it is substantially more resistant than the simple linear stack and requires less computation than the median stack. Because it is a nonlinear stack, one cannot write down a general transfer function for it, and even in the simplest of cases it is quite difficult to describe its behaviour. Consequently its behaviour has not previously been understood and most applications to date have been restricted to reducing the effects of incoherent noise spikes. The behaviour has now been strictly determined for several cases, including the asymptotic (large m) case. From these, its general behaviour may be determined, and is demonstrated in Figs 1 and 2 for synthetic and real data, respectively.

An *N*th-root stack gives a biased estimate at each point in the record, the bias being such that the expected result is less than the signal. Because it is nonlinear, the amount of bias depends in a complicated way on the signal-to-noise ratio (SNR), the number of channels, and the noise distribution, with the bias increasing as the SNR decreases.

This dependence on the SNR at each point on the waveform produces distortion (Fig. 1 d-f). Where the signal is very small signal destruction can occur, as exemplified by the destruction of the side-lobes, especially on the right-hand wavelet (Fig. 1e and 1f). However, the distortion usually has the effect of sharpening signal wavelets, so that it is actually easier to identify the presence of a genuine response. Note that the wavelet is sharpened without any time shift.

By far the most important property of the *N*th-root stack is that it exhibits a dynamic noise reduction. When the SNR is large, an *N*th-root stack is less effective in reducing the noise than a simple linear stack: if the variance of the noise is σ^2 then the variance of a linear stack is σ^2/m; and for an *N*th-root stack is slightly greater. However, this is relatively unimportant with a large SNR. When there is no signal, the variance of an *N*th-root stack decreases dramatically to σ^2/m^N; while the variance of a linear stack remains unchanged. Thus an *N*th-root stack provides very powerful suppression of background noise with reasonable noise

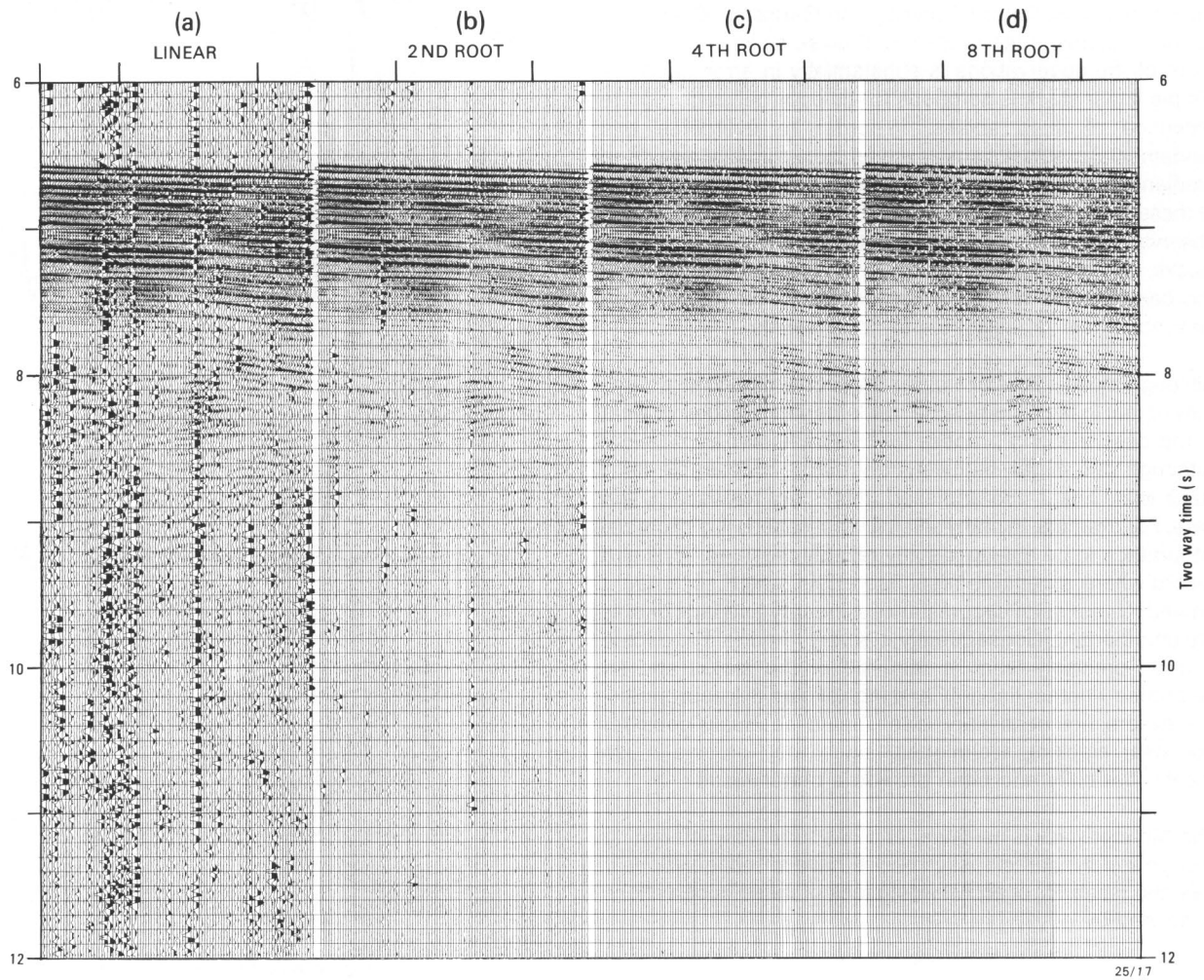

FIGURE 2
Stacks of 6-fold CDP reflection data from the Solomon Sea. (a) Linear stack, (b) 2nd-, (c) 4th-, and (d) 8th-root stacks. The data contain random bursts of noise on single channels. In all displays the amplitudes have been normalised for display purposes.

suppression in the presence of a signal. This dynamic noise reduction, together with the sharpening of wavelets, produces a large enhancement of the contrast between times when there is a signal, and times when there is not. This is especially evident (Fig. 1f), where the background noise in regions away from the wavelets is almost completely removed. Coupled with its resistance to noise spikes and its simplicity in implementation, this makes the *N*th-root stack a very powerful processing tool under the right circumstances.

Fig. 2 demonstrates the application of the *N*th-root stack to real, 6-fold seismic data that were contaminated by bursts of noise on single channels. Noise such as this behaves in the same way as spikes, and in the linear stack is still evident despite its 6-fold reduction. If a linear stack is to be used before further processing, extensive trace editing would be required. In the 2nd-root stack the noise is greatly reduced; in the 4th- and 8th-root stacks, it is effectively removed. Note also the sharpening of the reflection horizons exemplified by the narrowing of the infilled areas of the wavelets. The distortion for the 2nd- and 4th-root stacks is not great, indicating that even though the *N*th-root process is nonlinear, it does not necessarily restrict further processing.

References

Muirhead, K. J. (1968)—'Eliminating false alarms when detecting seismic events automatically', *Nature* **217,** 533–534.

A CASE STUDY OF THE SNAPPER GAS FIELD OFFSHORE GIPPSLAND

M. N. Megallaa and J. M. Ashworth

Introduction

The Victorian Department of Industry, Technology and Resources is currently carrying out a review of the Snapper Field gas reserves. The Snapper Field is a four-way ENE–WSW faulted anticline located 30 kms off the Gippsland coastline in an average water depth of 54 m (Fig. 1). The field was discovered by Esso-BHP in June 1968. To date six exploration wells (Snapper 1 to 6) and twenty-one development wells have been completed.

Part of the process for reviewing the reserves requires the mapping of the field's seismic grid (which consists of parts of G82B and reprocessed G77A surveys) on three fieldwide horizons. This paper considers the following in relation to the mapping:

1. A method of depth mapping which has been devised and tested to take into account problems associated with dip on the field's flanks.
2. Deviation between computed and observed seismic velocity data due to variations in the ground's heterogeneity.
3. The use of synthetic seismograms to relate seismic data to well control and the polarity reversal of seismic signals associated with direct hydrocarbon indication (DHI).

The study utilises the Department's GEOLOG (Mincom Pty) and SMC-GPC (ECS Pty Ltd) Packages. In addition, a special purpose inhouse depth conversion computer programme was written (Megallaa 1986).

Geology of Snapper Field

A gas cap overlying an oil leg occurs in the Snapper structure in the upper part of the Latrobe Group sediments of the Eocene 'N-1' palynological zone (based on Esso's palynological nomenclature). The Gas Oil Contact (G.O.C.) and Oil Water Contact (O.W.C.) are at depths of 1382 m and 1390 m respectively b.s.l. (Seage *et al.* 1985). The N-1 reservoir is sealed by the unconformably overlying marine mudstone of the Lakes Entrance Formation and the Gippsland Limestone Formation of the Seaspray Group (Fig. 2). The N-1 sediments consist of interbedded sandstone, siltstone, shale and coal. The reservoir sands are characteristic of braided stream and point bar deposition within a lower delta plain environment and have been subdivided into nine sandstone units (N-1.1 to N-1.9) which are separated by shales and coals of thicknesses up to 10 m. A glauconitic fine grained sandy and silty marine unit named the Gurnard Formation (N-1.0) unconformably overlies the top of the 'Coarse Clastics' (N-1.1).

Seismic Mapping

The Problem

The field's seismic velocity gradient increases with depth, becoming steeper on the flanks of the structure. The western flank is separated from the Whiting Field by a saddle (Fig. 4) over which the base of a deepening Miocene channel (Fig. 2), filled with high velocity limestone, adds another steep velocity gradient component. These two factors combined provide a depth conversion problem. It is in these areas, away from well control, where a reliable method of depth conversion is required.

Mapped Horizons

To calculate the volume of the reservoir, three horizons were mapped:

(a) **Top of the Latrobe Group N-1.0** (Figs 2, 4, 5) this corresponds to a strong negative reflection co-efficient (Fig. 3a) which produces a pronounced high amplitude, low frequency trough. The horizon's response is possibly caused by the presence of gas traces at the top of the Gurnard Formation.
(b) **Top of the N-1.4 Sand Unit** (Fig. 2); and
(c) **Top of the N-1.9 Sand Unit** (Fig. 2). The N-1.4 and N-1.9 have similar low frequency troughs corresponding to a strong negative reflection co-efficient generated from the top of relatively thick coal seams (Fig. 3a). They are